



Article

Verification of Optimal X-Ray Shielding Properties Based on Material Composition and Coating Design of Shielding Materials

Seon-Chil Kim ^{1,*} , Jae-Han Yun ², Hong-Sik Byun ³ and Jian Hou ^{4,*} 

¹ Department of Biomedical Engineering, School of Medicine, Keimyung University, 1095 Dalgubeol-daero, Daegu 42601, Republic of Korea

² Gyeongbuk Hybrid Technology Institute, Yeongcheon 38899, Republic of Korea; jyun@ghi.re.kr

³ Department of Chemical Engineering, Keimyung University, Daegu 42601, Republic of Korea; hsbyun@kmu.ac.kr

⁴ School of Intelligent Manufacturing, Luoyang Institute of Science and Technology, Luoyang 471023, China

* Correspondence: chil@kmu.ac.kr (S.-C.K.); jhou@lit.edu.cn (J.H.)

Abstract: Health care workers performing radiography on patients in hospitals typically wear aprons for radiation protection. Protective properties are achieved through a combination of shielding materials and polymers. Various shielding materials are mixed with polymers to prepare composite materials. Numerous methods have been devised to design and alter the composition of these materials to improve the shielding performance of aprons. In this study, the shielding performance was analyzed based on the arrangement of shielding materials, the composition of materials (mixed or single), and the fabrication design of the shielding sheets. Various shielding sheets were created using different arrangements of tungsten oxide, bismuth oxide, and barium sulfate, and their shielding efficacy was compared. The atomic number and density of the shielding material directly affect the shielding property. The effectiveness of the composite sheet increased by more than 5% when positioned close to the X-ray tube. Sheets fabricated from materials separated by type, rather than mixed, exhibited a greater X-ray shielding effectiveness because of their layered structure. Therefore, structural design considerations such as linings, outer layers, and inner layers of protective sheets should be considered for effective shielding in medical institutions.

Keywords: X-ray; radiation shielding; shielding sheet; tungsten oxide; bismuth oxide



Citation: Kim, S.-C.; Yun, J.-H.; Byun, H.-S.; Hou, J. Verification of Optimal X-Ray Shielding Properties Based on Material Composition and Coating Design of Shielding Materials.

Coatings **2024**, *14*, 1450. <https://doi.org/10.3390/coatings14111450>

Academic Editors: Panos Pouloupoulos and Gianni Barucca

Received: 27 September 2024

Revised: 25 October 2024

Accepted: 12 November 2024

Published: 14 November 2024



Copyright: © 2024 by the authors. Licensee MDPI, Basel, Switzerland. This article is an open access article distributed under the terms and conditions of the Creative Commons Attribution (CC BY) license (<https://creativecommons.org/licenses/by/4.0/>).

1. Introduction

Medical professionals performing procedures such as radiation diagnostic tests require various shielding tools for protection against radiation exposure [1]. Replacing lead, a heavy metal, with eco-friendly shielding materials is challenging due to lead's low cost and ease of processing [2,3]. Tungsten, an eco-friendly shielding material, exhibits a high density (19.25 g/cm³) and atomic mass (183.84) and is widely used as a lead substitute due to its excellent protective effects through numerous interactions with incident radiation [4,5]. However, tungsten's high melting point (3422 °C) and low affinity between particles restrict its ability to be mixed with other substances [6]. Therefore, when manufacturing shielding sheets from composite materials, a specific design that can effectively arrange the composition of the materials during the mixing process is required.

Radiation shielding in medical institutions and industries can be categorized into two objectives: protecting users and safeguarding devices or equipment. Shielding tools are typically fabricated in sheet and film forms [7]. Flexibility is crucial for shielding materials because shielding garments are worn by medical practitioners. Strength and processability are also essential for shielding films to block incoming energy from external sources [8]. Thus, shielding tools should satisfy weight, thickness, and rigidity requirements to achieve

the desired flexibility and strength [9]. The material composition for shielding tool design should be based on the properties required for the intended use. To ensure user mobility, processing techniques such as blending polymers with composite metal materials, which reduce weight and thickness, are typically used [10].

Typically, the manufacturing process for X-ray shielding sheets involves randomly mixing polymer materials with metal particles that have shielding capabilities, with the metal content presented as a percentage by weight (wt.%) of the total weight [11]. Although increasing the wt.% of metal materials improves shielding sheets' performance, this measure also increases their weight and can reduce their tensile strength and flexibility. To address this problem, considering that a certain amount of shielding material is necessary for maintaining functionality, a preferred approach is to design thin sheets with a thickness of 0.3 mm or less in a multilayer structure [6].

The arrangement of shielding substances should be considered when fabricating multilayer shielding sheets from composite materials. The amount of energy decreases with the distance from the radiation source to the target, resulting in various incident energy intensities. Generally, when interpreting the order of shielding materials based on the sum of densities, the commutativity of multiplication applies; that is, the order does not affect the outcome [12]. However, diagnostic X-rays, which have continuous and complex energies, exhibit changes in incident intensity as they pass through the shielding sheet. This variation could be attributed to differences in the densities and absorption coefficients of the materials inside the sheet, which affect shielding performance [13].

Therefore, in this study, experimental analyses were performed to study the arrangement design of the shielding material, which affects the time it takes for X-rays to reach the final detector, considerably affecting the performance of the shielding sheet. The objective was to find the optimal design conditions for radiation-shielding sheets. Additionally, we compared the shielding performance of sheets prepared using a single material and a mixture of multiple materials. Furthermore, we evaluated the effect of a multilayer structure on shielding performance based on experimental results.

Studies have focused on reducing the spacing between shielding material particles within the sheet structure. The results have revealed that the arrangement and positioning of particles considerably affects shielding performance, which is directly or indirectly related to density [14]. However, controlling the particle sizes of shielding materials during manufacturing is difficult because of their random arrangement; thus, specific shielding materials are used [15,16]. Among shielding materials, lead is a heavy metal that can adversely affect human health. Various eco-friendly materials, such as tungsten, barium sulfate, antimony, bismuth oxide, and tin, can be used as alternatives to lead [17]. In this study, tungsten was used as the primary shielding material, with barium sulfate and bismuth oxide added, which are commonly used as the outer layers or linings of shielding garments and nonwoven fabrics. We investigated the optimal arrangement of these materials for designing effective shielding garments [18–20].

We explored factors affecting the shielding performance of the selected materials, such as atomic number and density, in relation to the positioning of the entry and exit points of incident radiation for shielding sheets. We comparatively analyzed the shielding effects of sheets prepared by mixing two or more shielding materials versus using a single material. Internal particle structures were compared, and the shielding effectiveness for identical contents was verified. Additionally, we used eco-friendly shielding materials, tracked changes in shielding performance according to the internal material sequence of the shielding sheet, and proposed an optimal sequence pattern of shielding materials to create an effective radiation-shielding composite sheet. According to the study findings, shielding performance can be improved using materials with differentiated shielding properties for the linings and outer layers of aprons used by medical professionals in diagnostic settings.

2. Methods and Materials

The initial incident energy intensity is attenuated as radiation passes through a material [21]. When a multilayered shielding sheet is used, the shielding performance depends on the material properties and design information of composite materials. In a multilayer structure, as presented in Figure 1, the intensity depends on the thickness for layers with the same density. For a constant thickness, the intensity depends on the density of the shielding material. Moreover, the ratio of transmitted intensity to incident intensity can differ depending on the atomic number and absorption coefficient of the shielding material [22]. In this study, we manufactured prototypes using a combination of two or more materials and compared and assessed their shielding effectiveness based on the manufacturing composition and design.

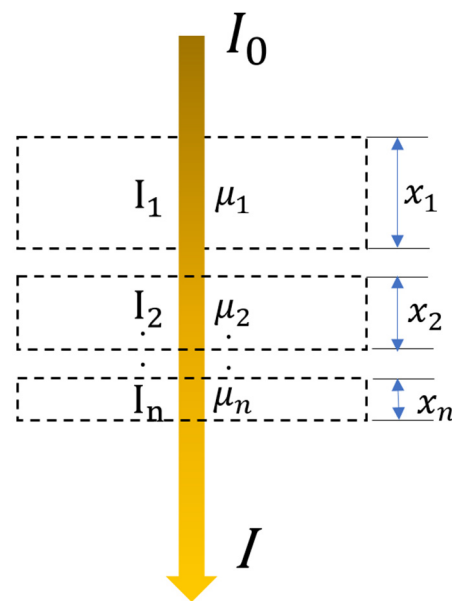


Figure 1. Shielding design based on radiation intensity (I_0 : incident intensity, I : transmitted intensity, μ : absorption coefficient, χ : thickness).

Incident radiation is attenuated based on the probability of interaction between photons and the mass per unit area of a specific medium and can be calculated using the Beer–Lambert law, as presented in Equation (1) [23]. Although shielding materials made from composite materials separated into layers and those made from single materials with a layered structure both have the same multilayer configuration, their shielding performances differ. Therefore, the radiation-shielding effectiveness is directly influenced by the density and thickness of the shielding material, which are determined by its chemical composition. For shielding materials with the same density, the attenuation intensity of incident radiation depends on thicknesses $\chi_1, \chi_2, \dots, \chi_3$. Thus, adjusting the thickness is the simplest method for producing radiation-shielding materials. For composite materials, the linear attenuation coefficient μ (cm^{-1}) is given by Equation (2), where ρ (g/cm^3) is the measured density of the shielding material and ω_i is the weight fraction. Therefore, the mass attenuation coefficient ($\frac{\mu}{\rho}$) for a compound or mixture of elements is given by Equation (2) [24]. In this context, the cross-sectional area of the incident radiation is the probability of interaction between the shielding material and incident radiation. Here, $\sum_i^n A_i \left(\frac{\mu}{\rho}\right)_i$ represents the molecular weight of the composite shielding material, and N_A is Avogadro's number. Therefore, the total effective electron cross section (σ_n), as detailed in Equation (3), indicates that higher atomic numbers lead to superior shielding efficiency [25].

$$I = I_0 e^{-(\mu x)_n} \quad (1)$$

$$\left(\frac{\mu}{\rho}\right)_n = \sum_i^n \omega_i (\mu/\rho)_i \quad (2)$$

$$\sigma_n = \frac{1}{N_A} \sum_i^n A_i \left(\frac{\mu}{\rho}\right)_i \quad (3)$$

$$\sigma_a = \frac{\mu/\rho}{N_A \sum_i^n \frac{\omega_i}{A_i}} \quad (4)$$

The arrangement of shielding materials for improved shielding performance is related to the effective atomic number. As presented in Equation (4), the total atomic effective cross-section (σ_a) can be evaluated using the mass attenuation coefficient. The ratio of the total electron cross-section (σ_n) to this value is referred to as the effective atomic number (Z_{eff}), as given by Equation (5) [26]. A higher effective atomic number results in a greater probability of interaction with incident radiation. Therefore, the incident radiation can be arranged based on the effective atomic number of the shielding material [27].

$$Z_{eff} = \frac{\sigma_a}{\sigma_n} \quad (5)$$

In the experiments, eco-friendly alternatives to lead were used as shielding materials. First, tungsten oxide (WO_3), with an elemental composition ratio of approximately 79.29% tungsten and 20.71% oxygen and an effective atomic number (Z_{eff}) of 38, was used. Tungsten, with an atomic number of 74 and a density of 19.25 g/cm^3 , is the most effective material to replace lead [28]. Barium sulfate (BaSO_4) has an elemental composition ratio of 58.84% barium, 13.74% sulfur, and 27.42% oxygen, with a Z_{eff} of 68, a density of 4.49 g/cm^3 , and a molar mass of 233.38 g/mol . Barium has an atomic number of 56.

Bismuth oxide (Bi_2O_3) has an elemental composition ratio of approximately 89.69% bismuth and 10.31% oxygen, with a Z_{eff} of 78, a density of 8.9 g/cm^3 , and a molar mass of 465.96 g/mol . Bismuth has an atomic number of 83 [29]. These three eco-friendly shielding materials are widely used as substitutes for lead. The evaluation of the shielding performance involved stacking the fabricated sheets in ascending order of density and arranging materials with higher atomic numbers according to the direction of the incident light.

For fabricating experimental shielding sheets, shielding materials (with a particle size of $100\text{--}400 \text{ }\mu\text{m}$) and a polymer substance, specifically high-density polyethylene (HDPE), were used [9,30–32]. Polyethylene with a molecular weight of over 4 million and a density of 0.91 g/cm^3 was selected. For the solid polymer, a casting solution was prepared using *N,N*-dimethylformamide (DMF, 99.5%) as the solvent. HDPE was dissolved in DMF (10 wt.%) in a mixer. The shielding material (80 wt.%) was then added to the prepared casting solution, and the mixture was stirred at 5000 rpm to disperse the particles. To eliminate voids within the shielding sheet, a plasticizer, diisononyl phthalate (DINP), was used at a concentration of 0.85–0.95 wt.%. To maintain the uniform shielding performance of the final casting solution, the substance was filtered and dried. A compression molding calendaring process was used to produce the final shielding sheet with dimensions of $300 \text{ mm} \times 300 \text{ mm} \times 0.3 \text{ mm}$ (Figure 2). In this study, two additional comparative experiments were conducted. First, sheets were produced by initially mixing three materials on a particle basis and then combining them with polyethylene in a second mixing step. The second type of sheet was made by mixing each material with polyethylene separately and then layering the three sheets to create a multilayer structure. Both types were produced with the same thickness to compare their shielding performance differences. Therefore, to determine the optimal conditions, the X-ray shielding effectiveness of the shielding sheets was tested based on their density and atomic number, using the same thickness and 80 wt.% content as the criteria for the experiments.

The particle dispersion within the shielding sheet was observed through optical microscopy using a field-emission scanning electron microscope (FESEM Hitachi S-4800, Hitachi High-Tech Corporation, Tokyo, Japan) by examining thin-film sections of the sheet [33]. The lead equivalent testing method (KS A 4025:1990, revised in 2009)—the exper-

imental method for evaluating the radiation-shielding performance—was applied as per the Korean Industrial Standard for X-ray shielding materials, as illustrated in Figure 3 [34]. To eliminate backscatter, the transmitted radiation dose was measured 70 cm from the floor, as depicted in Figure 3. We used an X-ray generator (Toshiba E7239, 150 kV-500 mA, 1999, Toshiba Corporation, Tokyo, Japan) to conduct 10 experiments and calculated the average of the measured doses. A DosiMax plus 1 dose detector (2019, IBA Dosimetry Corp., IBA Dosimetry Corp., Schwarzenbruck, Germany) was used after calibration and verification.

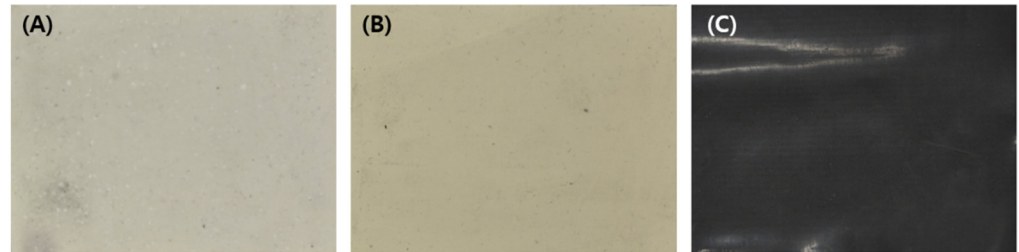


Figure 2. Shielding sheets of (A) barium sulfate, (B) bismuth oxide, and (C) tungsten oxide.

The shielding sheet performance was evaluated based on the shielding efficiency, considering the radiation protection efficiency (RPE) [35]. Equation (6) details the shielding efficiency of the radiation-shielding sheet in the experiment. The doses measured with and without the shielding sheet placed between the X-ray beam and detector are denoted as e and e_0 , respectively.

$$RPE = \left(1 - \frac{e}{e_0}\right) \times 100 \quad (6)$$

RPE = shielding factor, e_0 = incident dose (μR), and e = transmitted dose (μR).

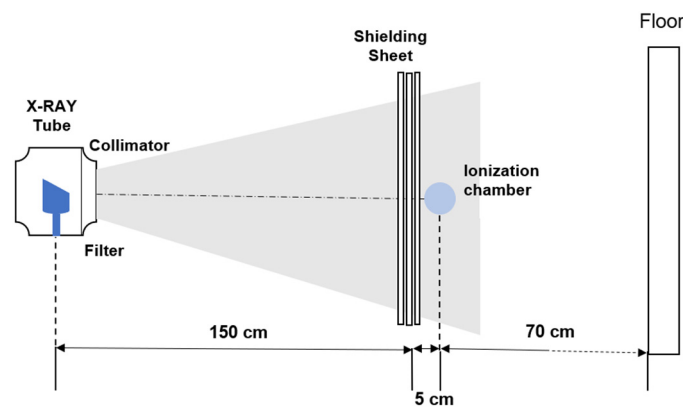


Figure 3. Evaluation of radiation-shielding performance of shielding sheets.

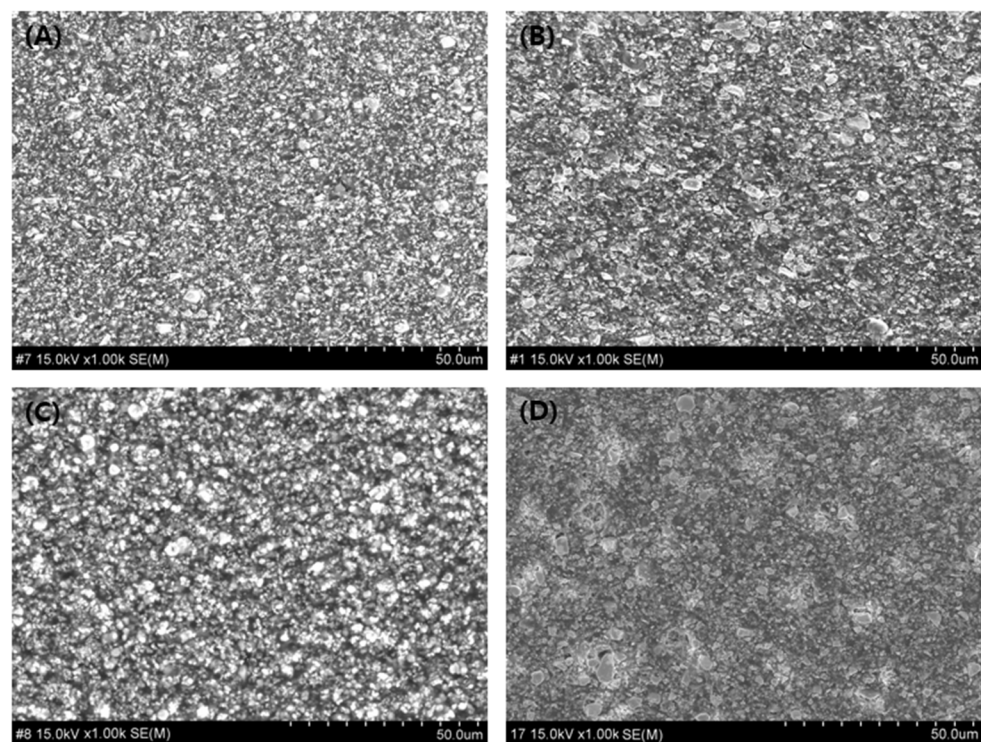
3. Results

The physical properties of the shielding sheets of each type are listed in Table 1. Tungsten oxide, bismuth oxide, and barium sulfate were used to manufacture the sheet. The properties of the array sheet (created by stacking three 0.3 mm sheets in sequence) and the mixed sheet (made by blending the three materials) are presented. Although the density of the sheets varied depending on the shielding material, the difference in density between the sheets made by compressing three sheets into one sheet and by mixing the materials was not significant. However, the density of the sheets depends on the material used. In the case of laminated sheets, the inclusion of an air layer resulted in differences in the relative thickness and density [36–38].

Table 1. Physical property analysis by type of sheet manufacturing.

Sheet Types	Weight (kg/m ²)	Thickness (mm)	Density (g/cm ³)
Barium sulfate (BaSO ₄)	3.1 ± 0.039	0.3 ± 0.010	10.333 ± 0.010
Bismuth oxide (Bi ₂ O ₃)	2.9 ± 0.030	0.3 ± 0.011	9.667 ± 0.021
Tungsten oxide (WO ₃)	2.7 ± 0.051	0.3 ± 0.012	9.766 ± 0.025
Array sheet (three sheets)	9.4 ± 0.011	1.1 ± 0.051	8.545 ± 0.032
Mixed sheets (one sheet)	8.6 ± 0.013	0.9 ± 0.012	9.556 ± 0.031

This difference in density is visually observable, as presented in Figure 4. Figure 4A represents tungsten oxide, Figure 4B represents bismuth oxide, and Figure 4C represents barium sulfate. The distribution state of the particles can be confirmed in the order of tungsten oxide, bismuth oxide, and barium sulfate. Figure 4D details the particle structure of the shielding sheet prepared by mixing the three materials. The gap between the particles is large, and the small particles are tightly packed. Therefore, the higher the affinity of the shielding material for the polymer substance, the more optimal the spacing between the particles. The closer the particle spacing is, the better the radiation-shielding effect is. Therefore, when the affinity between the shielding material and polymer substance is low, the use of a composite material is expected to be effective.

**Figure 4.** Shielding sheets manufactured using: (A) tungsten oxide, (B) bismuth oxide, (C) barium sulfate, and (D) mixed sheet.

The shielding sheets were arranged in order of density and atomic number to achieve a thickness of 0.3 mm. Their shielding effectiveness was compared to that of lead, which was considered the standard. In the first experiment, the shielding sheets were arranged in the order of tungsten oxide, bismuth oxide, and barium sulfate from the X-ray source to the detector, based on their density. Additionally, experiments were conducted by swapping the positions of the tungsten oxide and barium sulfate sheets. In the second experiment, the sheets were arranged in the order of bismuth oxide, tungsten oxide, and barium sulfate, from the highest to the lowest atomic number. Next, the sheets were arranged in reverse order. The shielding performance results are listed in Table 2. The

shielding was most effective when materials with higher atomic numbers and densities were positioned toward the X-ray source. By contrast, in the case of elements with lower atomic numbers and densities, the shielding performance was approximately 5%–6% lower. This phenomenon demonstrates that the shielding performance improved with a higher probability of interaction with electrons during the incidence process.

Table 2. Shielding performance based on density and atomic number (thickness: 0.3 mm).

X-Ray Tube Voltage (kVp)	RPE (%) ± SD (%)				
	Lead	W/Bi/Ba	Ba/Bi/W	Bi/W/Ba	Ba/W/Bi
40	100 ± 0.2	96 ± 0.1	91 ± 0.0	91 ± 0.2	90 ± 0.0
60	98 ± 0.0	93 ± 0.2	88 ± 0.2	89 ± 0.0	88 ± 0.3
80	95 ± 0.0	89 ± 0.0	85 ± 0.0	84 ± 0.1	84 ± 0.1
100	94 ± 0.1	85 ± 0.0	80 ± 0.0	78 ± 0.1	78 ± 0.1
120	91 ± 0.0	82 ± 0.2	78 ± 0.3	75 ± 0.0	76 ± 0.2

kVp = kilovoltage peak, with the X-ray source 155 cm away from the dosimeter.

The shielding performances of three single sheets made from each of the three shielding materials and the composite sheet made by mixing the three materials were compared with that of lead as a standard. According to the results of the study, summarized in Table 3, the shielding performance of the sheets prepared by mixing the three shielding materials was the lowest.

Table 3. Comparison of shielding performance between single materials and composite materials (thickness: 0.3 mm).

Tube Voltage (kVp)	RPE (%)				
	W	Bi	Ba	Mixed Sheet W/Bi/Ba	Lead
40	96 ± 0.2	85 ± 0.1	78 ± 0.0	92 ± 0.1	100 ± 0.0
60	95 ± 0.0	82 ± 0.0	75 ± 0.0	88 ± 0.2	98 ± 0.2
80	92 ± 0.1	78 ± 0.1	70 ± 0.2	84 ± 0.1	95 ± 0.1
100	91 ± 0.0	75 ± 0.1	68 ± 0.0	80 ± 0.0	94 ± 0.1
120	90 ± 0.2	70 ± 0.0	60 ± 0.1	74 ± 0.0	91 ± 0.0

kVp = kilovoltage peak, with the X-ray source 155 cm away from the dosimeter.

Additionally, the shielding performance of a single sheet made by combining three 0.1 mm sheets (each from one of the three materials) was compared with the performance of a 0.3 mm composite sheet made from the three materials, as presented in Table 4. The multilayer structure of individually manufactured shielding sheets exhibited a slightly improved shielding performance compared with that of the shielding sheets of mixed materials. In all the experimental results, the shielding performance (RPE) demonstrated an excellent accuracy with a relative error less than 1%.

Table 4. Comparison of shielding performance between composite materials and compressed sheets (thickness: 0.3 mm).

Tube Voltage (kVp)	RPE (%)		
	Mixed Sheet	Single Material Sheets	Lead
40	94 ± 0.0	96 ± 0.1	100 ± 0.2
60	90 ± 0.1	93 ± 0.0	98 ± 0.0
80	87 ± 0.1	89 ± 0.1	95 ± 0.0
100	85 ± 0.2	85 ± 0.0	94 ± 0.1
120	84 ± 0.0	82 ± 0.0	91 ± 0.0

kVp = kilovoltage peak, with the X-ray source 155 cm away from the dosimeter.

4. Discussion

When multiple shielding materials are mixed during the fabrication of shielding sheets, achieving a uniform particle size in the internal design becomes challenging owing to the physical properties of the particles. Although producing particles of uniform nanometer size using single materials for shielding sheets is possible, stability in particle processing and the cost-effectiveness of the final product are significant concerns in large-scale production [39]. Therefore, in composite materials, particles of different sizes are combined with polymers. This variation in the particle size can occasionally reduce gaps between particles, increasing the density. However, most cases require process technologies, such as bubble removal during mixing and the addition of additives [40].

In this study, we investigated whether it is more advantageous to create single-material sheets that are then assembled into a multilayer composite sheet or to mix materials to produce a single composite sheet for effective shielding performance. Although no significant difference was observed, using single materials proved to be more effective for medical radiation shielding. Shielding involves interactions such as absorption and scattering, which can prevent unidirectional transmission. Therefore, arranging particles with uniform properties is beneficial for achieving effective shielding.

Additionally, arranging the sheets fabricated from single materials with higher atomic numbers and densities to face the radiation source improves their shielding performance. This arrangement results in increased interactions with the incident photon energy and is similar to using high-density elements for radiation shielding. By applying the principle of graded-Z shielding, the combination of W/Bi/Ba presents considerable potential for independent shielding, due to having effective atomic numbers [41–43]. To enhance shielding performance, the electron density at the contact area should be increased by increasing the contact area with incident radiation or material density [44]. Thus, for the production of shielding sheets, either specifying a single material that satisfies the conditions or presenting the structural conditions of a composite material is crucial.

In this study, instead of using conventional methods for particle dispersion and layering structures, we considered the organizational arrangement of the shielding materials. Placing materials with higher atomic numbers and densities near the initial contact point with incident radiation can enhance shielding effectiveness. The results indicated that the arrangement of materials in the shielding sheet is crucial for designing shielding aprons used in medical institutions. Placing tungsten near the radiation source was the most effective arrangement, followed by the placement of bismuth and barium sulfate. The arrangement of shielding materials affects shielding performance based on the particle ratio during the mixing process. In particular, when not using a single material, the arrangement of shielding materials that can achieve the desired performance is a critical factor in radiation defense design. Therefore, a multilayer structure is more effective for radiation shielding than a single-layer structure, highlighting the importance of material composition and design in multilayer structures.

To enhance shielding performance, a composite structure of single-material sheets is more effective than mixed materials in various combinations. This approach can significantly contribute to the development of diverse shielding products. This study verified the role of material composition and arrangement in the design of various composites and applied these findings to medical radiation shielding.

5. Conclusions

When manufacturing X-ray shielding sheets for medical institutions, the composition design of each material affects the shielding performance. When a multilayer structure is created by positioning materials with higher atomic numbers and densities toward the X-ray source, the shielding performance is improved by approximately 5%–6% compared with sheets arranged with the opposite configuration. Furthermore, experimental results have revealed that multilayer sheets made with separated shielding materials are more effective than sheets in which materials are mixed before being combined with polymers.

This phenomenon indicates that such findings could be beneficial for the design of shielding layers, linings, and outer layers in protective clothing used in medical settings.

Author Contributions: S.-C.K. was responsible for the original draft, reviewing and editing the manuscript, investigation, data curation, project administration, and the formal analysis. J.-H.Y. contributed resources and was involved in funding acquisition, the study's methodology, and the validation of the results. H.-S.B. conceived and supervised the study and was responsible for project administration. J.H. was responsible for the study's methodology, the validation of the results, and investigation. All authors have read and agreed to the published version of the manuscript.

Funding: This work was funded by a National Research Foundation of Korea (NRF) grant from by the Korea government (MSIT) (NRF 2020R1I1A3070451).

Institutional Review Board Statement: Not applicable.

Informed Consent Statement: Not applicable.

Data Availability Statement: All data generated during this study are included in this manuscript.

Conflicts of Interest: The authors declare no conflicts of interest.

References

1. Boice, J., Jr.; Dauer, L.T.; Kase, K.R.; Mettler, F.A., Jr.; Vetter, R.J. Evolution of radiation protection for medical workers. *Br. J. Radiol.* **2020**, *93*, 20200282. [[CrossRef](#)] [[PubMed](#)]
2. Abualroos, N.J.; Baharul Amin, N.A.B.; Zainon, R. Conventional and new lead-free radiation shielding materials for radiation protection in nuclear medicine: A review. *Radiat. Phys. Chem.* **2019**, *165*, 108439. [[CrossRef](#)]
3. Boeykens, S.P.; Redondo, N.; Obeso, R.A.; Caracciolo, N.; Vázquez, C. Chromium and Lead adsorption by avocado seed biomass study through the use of Total Reflection X-ray fluorescence analysis. *Appl. Radiat. Isot.* **2019**, *153*, 108809. [[CrossRef](#)]
4. de Souza, A.C.; Aristone, F.; Gouvea, A.F.G.; Fernandes, H.B.; Miyai, A.; Rossi, J. Characterization and measurement of gamma radiation shielding of a new tungsten-lignin composite. *J. Compos. Mater.* **2021**, *55*, 3579–3588. [[CrossRef](#)]
5. Palanisami, S.; Dhandapani, V.S.; Jayachandran, V.; Muniappan, E.; Park, D.; Kim, B.; Govindasami, K. Investigation on physico chemical and X-ray shielding performance of zinc doped nano-WO₃ epoxy composite for light weight lead free aprons. *Materials* **2023**, *16*, 3866. [[CrossRef](#)]
6. Kepezshinskas, P.; Berdnikov, N.; Konovalova, N.; Kepezshinskas, N.; Krutikova, V.; Kirichenko, E. Native metals and alloys in trachytes and Shoshonite from the continental United States and high-K dacite from the Bolivian Andes: Magmatic origins of ore metals in convergent and within-plate tectonic settings. *Russ. J. Pac. Geol.* **2022**, *16*, 405–426. [[CrossRef](#)]
7. Kim, H.; Lim, J.; Kim, J.; Lee, J.; Seo, Y. Multilayer structuring of nonleaded metal (BiSn)/polymer/tungsten composites for enhanced γ -ray shielding. *Adv. Eng. Mater.* **2020**, *22*, 1901448. [[CrossRef](#)]
8. Kalkornsurapranee, E.; Kothan, S.; Intom, S.; Johns, J.; Kaewjaeng, S.; Kedkaew, C.; Chaiphaksa, W.; Sareein, T.; Kaewkhao, J. Wearable and flexible radiation shielding natural rubber composites: Effect of different radiation shielding fillers. *Radiat. Phys. Chem.* **2021**, *179*, 109261. [[CrossRef](#)]
9. Okafor, C.E.; Okonkwo, U.C.; Okokpujie, I.P. Trends in reinforced composite design for ionizing radiation shielding applications: A review. *J. Mater. Sci.* **2021**, *56*, 11631–11655. [[CrossRef](#)]
10. Li, Z.; Zhou, W.; Zhang, X.; Gao, Y.; Guo, S. High-efficiency, flexibility and lead-free X-ray shielding multilayered polymer composites: Layered structure design and shielding mechanism. *Sci. Rep.* **2021**, *11*, 4384. [[CrossRef](#)]
11. Almurayshid, M.; Alsagabi, S.; Alssalim, Y.; Alotaibi, Z.; Almsalam, R. Feasibility of polymer-based composite materials as radiation shield. *Radiat. Phys. Chem.* **2021**, *183*, 109425. [[CrossRef](#)]
12. Arif Sazali, M.; Alang Md Rashid, N.K.; Hamzah, K. A review on multilayer radiation shielding. *IOP Conf. Ser. Mater. Sci. Eng.* **2019**, *555*, 012008. [[CrossRef](#)]
13. Hussein, K.I.; Alqahtani, M.S.; Grelowska, I.; Reben, M.; Afifi, H.; Zahran, H.; Yaha, I.S.; Yousef, E.S. Optically transparent glass modified with metal oxides for X-rays and gamma rays shielding material. *J. X-Ray Sci. Technol.* **2021**, *29*, 331–345. [[CrossRef](#)]
14. Li, Q.; Wei, Q.; Zheng, W.; Zheng, Y.; Okosi, N.; Wang, Z.; Su, M. Enhanced radiation shielding with conformal light-weight nanoparticle-polymer composite. *ACS Appl. Mater. Interfaces* **2018**, *10*, 35510–35515. [[CrossRef](#)] [[PubMed](#)]
15. Gholamzadeh, L.; Asari-Shik, N.; Aminian, M.K.; Ghasemi-Nejad, M. A study of the shielding performance of fibers coated with high-Z oxides against ionizing radiations. *Nucl. Instrum. Method Phys. Res. Sect. A* **2020**, *973*, 164174. [[CrossRef](#)]
16. More, C.V.; Alsayed, Z.; Badawi, M.S.; Thabet, A.A.; Pawar, P.P. Polymeric composite materials for radiation shielding: A review. *Environ. Chem. Lett.* **2021**, *19*, 2057–2090. [[CrossRef](#)]

17. Guo-hui, W.; Man-li, H.; Fan-chao, C.; Jun-dong, F.; Yao-dong, D. Enhancement of flame retardancy and radiation shielding properties of ethylene vinyl acetate based radiation shielding composites by EB irradiation. *Prog. Nucl. Energy* **2019**, *112*, 225–232. [[CrossRef](#)]
18. Liang, D.; Shen, F.; Bao, Z.; Liu, Y.; Li, H. Research on textile materials for X-ray shielding. *E3S Web Conf.* **2021**, *290*, 01013. [[CrossRef](#)]
19. Wasel, O.; Freeman, J.L. Comparative assessment of tungsten toxicity in the absence or presence of other metals. *Toxics* **2018**, *6*, 66. [[CrossRef](#)]
20. Iwamiya, Y.; Kawai, M. Tungsten-coated cloth for radiation shielding made with the SilicaTech® coating technique. In Proceedings of the 14th International Workshop on Spallation Materials Technology (JAPAN), Fukushima, Japan, 11–16 November 2020. [[CrossRef](#)]
21. Agar, O.; Sayyed, M.I.; Akman, F.; Tekin, H.O.; Kaçal, M.R. An extensive investigation on gamma ray shielding features of Pd/Ag-based alloys. *Nucl. Eng. Technol.* **2019**, *51*, 853–859. [[CrossRef](#)]
22. Akman, F.; Kaçal, M.R.; Sayyed, M.I.; Karataş, H.A. Study of gamma radiation attenuation properties of some selected ternary alloys. *J. Alloys Compd.* **2019**, *782*, 315–322. [[CrossRef](#)]
23. Oshina, I.; Spigulis, J. Beer–Lambert law for optical tissue diagnostics: Current state of the art and the main limitations. *J. Biomed. Opt.* **2021**, *26*, 100901. [[CrossRef](#)]
24. Özpolat, Ö.F.; Alim, B.; Şakar, E.; Büyükyıldız, M.; Kurudirek, M. Phy-X/ZeXTRa: A software for robust calculation of effective atomic numbers for photon, electron, proton, alpha particle, and carbon ion interactions. *Radiat. Environ. Biophys.* **2020**, *59*, 321–329. [[CrossRef](#)]
25. Kaur, B.; Rani, N.; Vermani, Y.K.; Singh, T. Assigning effective atomic number and electron density for some lanthanide oxides over wide gamma-rays energies. *AIP Conf. Proc.* **2019**, *2142*, 120005. [[CrossRef](#)]
26. Kılıçoğlu, Ö. An investigation on effective atomic numbers and mass attenuation coefficients of some bioactive glasses. *Eur. J. Sci. Technol.* **2019**, *15*, 168–175. [[CrossRef](#)]
27. D'Souza, A.N.; Prabhu, N.S.; Sharmila, K.; Sayyed, M.I.; Somshekarappa, H.M.; Lakshminarayana, G.; Mandal, S.; Kamath, S.D. Role of Bi₂O₃ in altering the structural, optical, mechanical, radiation shielding and thermoluminescence properties of heavy metal oxide borosilicate glasses. *J. Non-Cryst. Solids* **2020**, *542*, 120136. [[CrossRef](#)]
28. Safari, A.; Rafie, P.; Taeb, S.; Najafi, M.; Mortazavi, S.M.J. Development of lead-free materials for radiation shielding in medical settings: A review. *J. Biomed. Phys. Eng.* **2024**, *14*, 229–244. [[CrossRef](#)] [[PubMed](#)]
29. Thumwong, A.; Chinnawet, M.; Intarasena, P.; Rattanapongs, C.; Tokonami, S.; Ishikawa, T.; Saenboonruang, K. A comparative study on X-ray shielding and mechanical properties of natural rubber latex nanocomposites containing Bi₂O₃ or BaSO₄: Experimental and numerical determination. *Polymers* **2022**, *14*, 3654. [[CrossRef](#)]
30. E, J.J.; Panneerselvam, K. Investigation on the influence of tungsten particulate in mechanical and thermal properties of HD50MA180 high density polyethylene composites. *Mater. Res. Express* **2020**, *7*, 045306. [[CrossRef](#)]
31. Obeid, A.; El, B.H.; El, S.O.; Alsayed, Z.; Awad, R.; Badawi, M.S. Effects of different nano size and bulk WO₃ enriched by HDPE composites on attenuation of the X-ray narrow spectrum. *Nucl. Technol. Radiat. Prot.* **2021**, *36*, 315–328. [[CrossRef](#)]
32. Abdolazadeh, T.; Morshedian, J.; Ahmadi, S. Preparation and characterization of nano WO₃/Bi₂O₃/GO and BaSO₄/GO dispersed HDPE composites for X-ray shielding application. *Polyolefins J.* **2022**, *9*, 73–83. [[CrossRef](#)]
33. Liang, X.; Gao, G.; Wu, G. Statistical analysis on hollow and core-shell structured vanadium oxide microspheres as cathode materials for lithium ion batteries. *Data Brief* **2018**, *18*, 719–722. [[CrossRef](#)] [[PubMed](#)]
34. Korean Standards Association. *Testing Method of Lead Equivalent for X-Ray Protective Devices*; Korean Standards Association: Seoul, Republic of Korea, 2017; Volume 17, p. 4025.
35. AlMisned, G.; Akman, F.; AbuShanab, W.S.; Tekin, H.O.; Kaçal, M.R.; Issa, S.A.M.; Polat, H.; Oltulu, M.; Ene, A.; Zakaly, H.M.H. Novel Cu/Zn Reinforced Polymer Composites: Experimental Characterization for Radiation Protection Efficiency (RPE) and Shielding Properties for Alpha, Proton, Neutron, and Gamma Radiations. *Polymers* **2021**, *13*, 3157. [[CrossRef](#)]
36. Zhang, H.; Lin, S. Research progress with membrane shielding materials for electromagnetic/radiation contamination. *Membranes* **2023**, *13*, 315. [[CrossRef](#)]
37. Vignesh, S.; Winowlin Jappes, J.T.; Nagaveena, S.; Krishna Sharma, R.; Adam Khan, M.; More, C.V.; Rajini, N.; Varol, T. Development of lightweight polymer laminates for radiation shielding and electronics applications. *Int. J. Polym. Sci.* **2022**, *2022*, 5252528. [[CrossRef](#)]
38. Budumuru, S.; Rao, S.S.; Jenjeti, D.; Suri Apparao, T.V. Shielding effectiveness of multilayer laminate of aluminum metal matrix and micro absorbing materials. *MethodsX* **2023**, *10*, 102172. [[CrossRef](#)] [[PubMed](#)]
39. Liang, C.; Gu, Z.; Zhang, Y.; Ma, Z.; Qiu, H.; Gu, J. Structural design strategies of polymer matrix composites for electromagnetic interference shielding: A review. *Nanomicro Lett.* **2021**, *13*, 181. [[CrossRef](#)]
40. Gilys, L.; Griškoniš, E.; Griškevičius, P.; Adlienė, D. Lead free multilayered polymer composites for radiation shielding. *Polymers* **2022**, *14*, 1696. [[CrossRef](#)]
41. Fan, W.C.; Drumm, C.R.; Roeske, S.B.; Scrivner, G.J. Shielding considerations for satellite microelectronics. *IEEE Trans. Nucl. Sci.* **1996**, *43*, 2790–2796. [[CrossRef](#)]
42. Klamm, B. Passive space radiation shielding: Mass and volume optimization of tungsten-doped polyphenolic and polyethylene resins. In Proceedings of the 29th Annual AIAA/USU Conference on Small Satellites, Logan, UT, USA, 8–13 August 2015.

43. Li, X.; Warden, D.; Bayazitoglu, Y. Analysis to evaluate multilayer shielding of galactic cosmic rays. *J. Thermophys. Heat Transf.* **2018**, *32*, 525–531. [[CrossRef](#)]
44. Chang, Q.; Guo, S.; Zhang, X. Radiation shielding polymer composites: Ray-interaction mechanism, structural design, manufacture and biomedical applications. *Mater. Des.* **2023**, *233*, 112253. [[CrossRef](#)]

Disclaimer/Publisher's Note: The statements, opinions and data contained in all publications are solely those of the individual author(s) and contributor(s) and not of MDPI and/or the editor(s). MDPI and/or the editor(s) disclaim responsibility for any injury to people or property resulting from any ideas, methods, instructions or products referred to in the content.